ESD-TR-77-280

Project Report

ETS-25

A CCD Radiometer for Use in GEODSS

F. L. McNamara
W. E. Krag

4 November 1977

Prepared for the Department of the Air Force
under Electronic Systems Division Contract F19628-78-C-0002 by

Lincoln Laboratory
MASSACHUSETTS INSTITUTE OF TECHNOLOGY
LEXINGTON, MASSACHUSETTS

The work reported in this document was performed at Lincoln Laboratory, a center for research operated by Massachusetts Institute of Technology, with the support of the Department of the Air Force under Contract F19628-78-C-0002.

This technical report has been reviewed and is approved for publication.

FOR THE COMMANDER

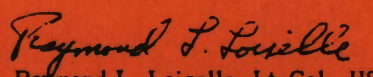

Raymond L. Loiselle, Lt. Col., USAF
Chief, ESD Lincoln Laboratory Project Office

MASSACHUSETTS INSTITUTE OF TECHNOLOGY

LINCOLN LABORATORY

A CCD RADIOMETER FOR USE IN GEODSS

F. L. McNAMARA
W. E. KRAG
Group 94

PROJECT REPORT ETS-25

4 NOVEMBER 1977

LEXINGTON MASSACHUSETTS

ABSTRACT

Proposed is a CCD radiometer for application in the GEODSS Program. An analysis is made of the predicted performance in a field environment. The results are compared for a variety of satellite brightnesses and levels of night sky background with the present single cell GaAs radiometer undergoing tests at the GEODSS Experimental Test Facility at White Sands Missile Range, New Mexico and with the Robinson-Wampler multi-channel radiometer in use at Lick Observatory, University of California, Santa Cruz, California, and the McDonald Observatory, University of Texas, Fort Davis, Texas. The comparison indicates that the CCD radiometer allows the optical signature of objects to be determined with higher accuracy and improved time resolution, and permits a more efficient utilization of telescope time.

TABLE OF CONTENTS

I. INTRODUCTION

Astronomers have widely used single detector photometers/radiometers as photon counting devices to measure the radiant intensity of stars and other celestial objects. It is planned to install a radiometer of this type at the GEODSS Experimental Test Site (ETS) for measuring satellite characteristics. As discussed below, single cell radiometers, while suitable for measuring the intensity of bright sources, have serious limitations when the sources are very faint or the night sky background (NSB) level is high.

A multi-channel or area radiometer designed by Wampler and Robinson[1,2] and successfully employed at Lick Observatory, University of California and more recently at McDonald Observatory,[3,4] University of Texas appears to be a more suitable device for measurements under the above mentioned conditions. The instrument, which is quite sophisticated, employs three stages of light intensification followed by an image dissector tube. However, measurement accuracy and flexibility are limited by afterglow on the phosphor screen of the final intensifier tube which can produce unwanted signals for long periods of time after the object of interest has left the field of view of the instrument.

Use of a CCD array as a radiometer preserves all of the advantages of the multi-channel radiometer without possessing the serious problem of phosphor afterglow. For this application, requirements on the number of elements in the CCD array are very modest and well within the state of the art. In fact small arrays suitable for this purpose have been made and tested by the Micro-Electronics Group in Division VIII.

The following analysis shows that the CCD radiometer: 1) in general shortens the integration time required to measure the intensity of an object, and 2) enables the background to be measured simultaneously. These permit a higher utilization of telescope time and the determination of optical signatures with higher accuracy and improved time resolution. The latter is of particular interest for those sources whose optical signature exhibits intensity variations. We recommend that a CCD radiometer be built and tested for future incorporation into the GEODSS System.

A comparison of the proposed CCD radiometer with a single cell diaphragm radiometer and the Wampler-Robinson device is given below.

II. THE SINGLE CELL RADIOMETER

The basic elements of the single cell radiometer are shown in Figure 1. The field of view of the detector is defined by a small aperture in a diaphragm which is imaged on the detector by a field lens. Filters can be introduced into the light path to select the spectral bandwidth of the radiation allowed to reach the detector. The output signal from the detector consists of a contribution from the night sky background as well as from any objects which may be in the field of view.

When used to measure intensity of an object in space the aperture which defines the field of view of the detector must be made large enough to allow for the spread in the image size when the light path through the atmosphere is degraded by turbulence. For a star, the point source image measured at the half power points can vary from about 5 microradians ($\sim$1 arc-second) under good seeing conditions to about 30 times that value under the poorest conditions. The seeing can vary during an evening as well as from night to night. To capture all of the energy contained within the image, the aperture must be wide enough to include the entire image profile, which to a first approximation can be assumed to be gaussian. Figure 2 gives typical image profiles normalized to unit area.

A further consideration in selecting the aperture size is the image wander introduced by the limited accuracy attainable by the pointing system. This depends on a number of factors including the precision of the servo and tracking systems as well as the accuracy to which the ephemeris of the object is known when blind tracking is employed.

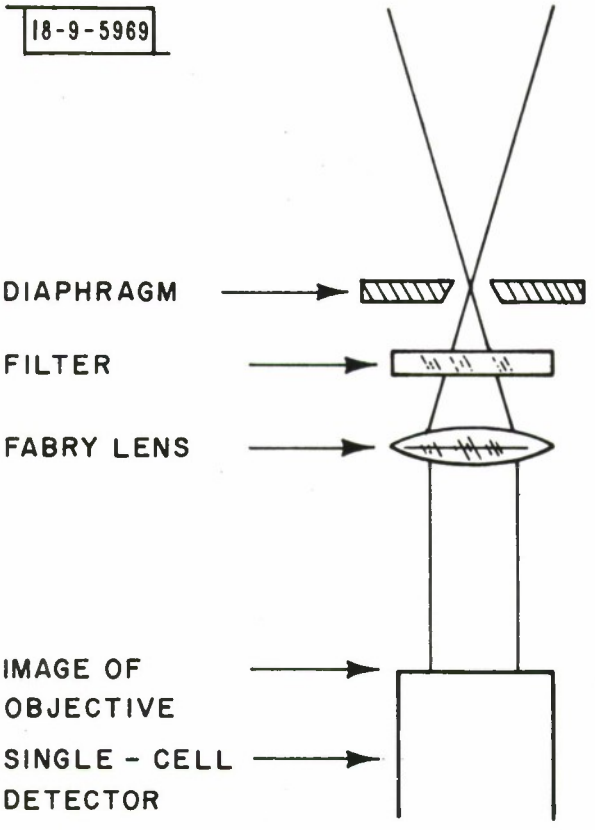

Fig. 1. Elements of a single cell photometer.

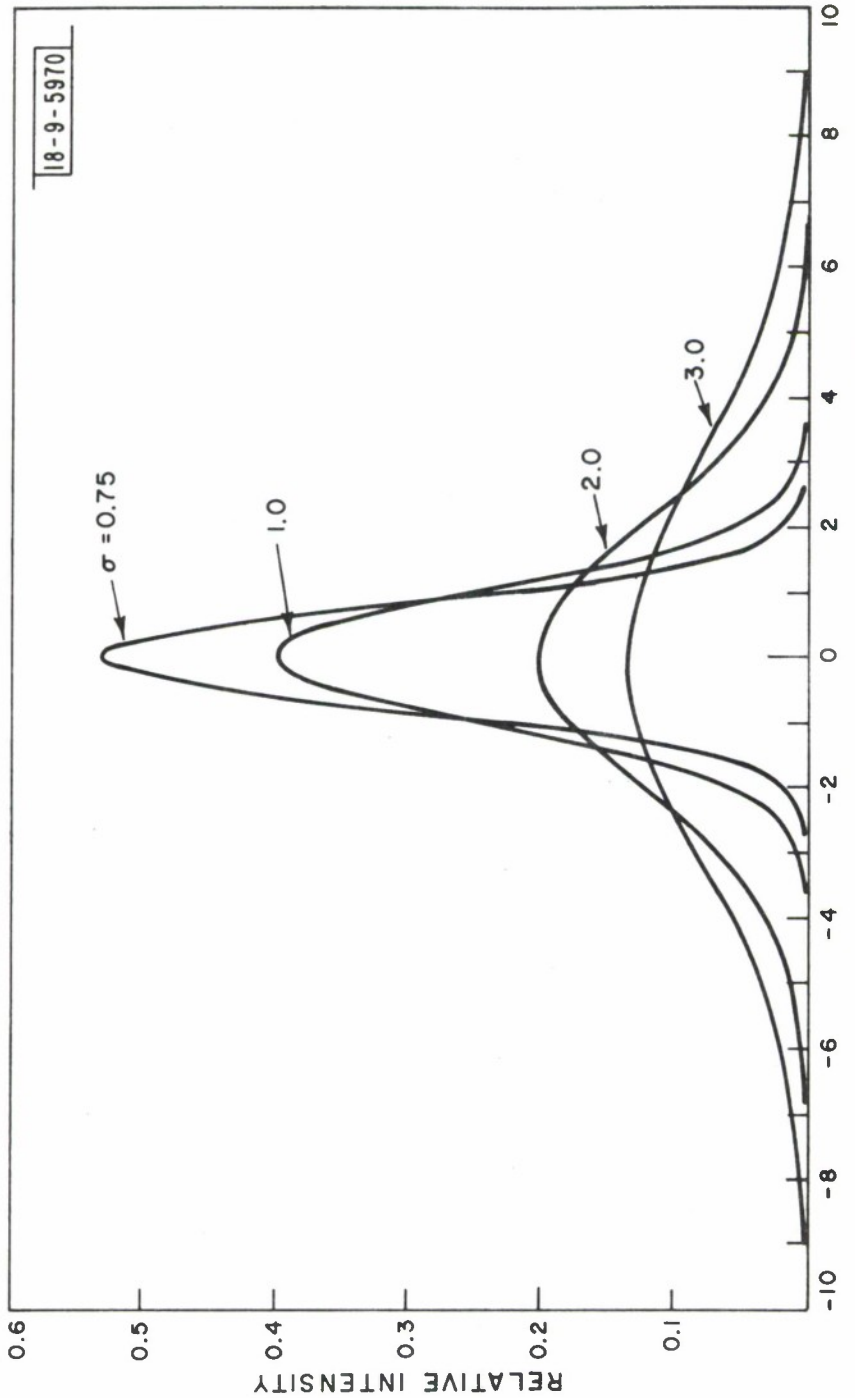

Fig. 2. Typical Gaussian profiles normalized to unit area.

When the instrument is used to determine the intensity of a single object in the field of view, the total photon count from the signal and background is measured. Therefore, an equal time must be spent on a NSB measurement to determine its contribution so that it can be subtracted from the total signal count. This, of course, doubles the measurement time and reduces the telescope utilization efficiency accordingly. Care must be taken in the manner in which the background is sampled during a measurement in order to minimize the errors which can be introduced by gradients and inhomogenities in the background.

For objects which are relatively bright against the night sky background, instruments of this type have been used with high accuracy to determine broadband and spectral intensities of these sources. For objects faint enough to have the background signal predominate the accuracy becomes severely limited.

III. SINGLE CELL RADIOMETER FOR GEODSS

A single cell radiometer employing a GaAs photomultiplier (PMT) has been designed for use with the 31-inch telescope at the ETS. Light from the object being measured is centered in the diaphragm aperture in front of the PMT by a half silvered pellicle mirror located in the central portion of the light path. The aperture diameter, ℓ, is expected to be fairly large, on the order of 0.030 inch, which results in an angular field of view, θ, of about 40 arc-seconds, since

$$\theta = \frac{\ell}{f} = \frac{0.030 \text{ rad}}{155} \times \frac{360 \text{ deg}}{2\pi \text{ rad}} \; 3600 \frac{\text{arc-sec}}{\text{deg}} = 40 \text{ arc-sec}$$

where f is the focal length of the 31-inch telescope in the cassegrain configuration. The aperture allows the detector to view an area (α^2) in space corresponding to about 1250 arc-sec^2.

For zero atmospheric attenuation an object of zero magnitude produces an irradiance[5] at the telescope aperture of 5×10^{10} photons/m^2/sec. For a 31-inch aperture ($A = 0.49 m^2$) telescope with a transmission through the instrument of 0.6 the number of photons incident on the detector per second is 1.47×10^{10}. If we further assume that the average quantum efficiency, q, over the spectral band of the sun is about 15% as given by Weber[6] the number of photoelectrons produced is 2.21×10^9/sec. Table I gives the photon flux density and photoelectrons produced for different values of night sky background (NSB).

TABLE I

Photon flux density, photon flux incident on the detector, and the number of photoelectrons produced by a GaAs detector for different values of night sky background (NSB) measured in equivalent stellar magnitudes/arc-sec^2, and for the given telescope parameters.

NSB	Aperture Irradiance (Photons/m^2/arc-sec^2/ sec)	Photons/Sec Incident on Detector (Telescope A = 0.49m^2, Telescope Transmission 0.6)	Photoelectrons Produced per arc-sec^2 / sec (q= 0.15)
17.5^m/arc-sec^2	5 x 10^3	1.47 x 10^3	221
18.0^m/arc-sec^2	3.15 x 10^3	9.26 x 10^2	139
20.0^m/arc-sec^2	5 x 10^2	1.47 x 10^2	22.1
21.0^m/arc-sec^2	2 x 10^2	58.5	8.8

The expression for the signal to noise ratio, SNR, is

$$SNR = \frac{\phi_e}{\left[\phi_e + \phi_{NSB} + N_I^2 \right]^{1/2}}$$

where ϕ_e is the number of detected photoelectrons from the object, ϕ_{NSB} is the number of detected photoelectrons from the NSB, and N_I is the number of noise electrons. For the GaAs photometer, N_I is small in comparison with ϕ_e or ϕ_{NSB}.

Now

$$\phi_e = \psi_{obj}\ a\ q\ t$$

$$\phi_{NSB} = \psi_{NSB}\ a\ q\ t\ \alpha^2$$

where ψ_{obj} and ψ_{NSB} are the photon flux densities at the aperture due to the object and NSB respectively, t is the integration time, q is the quantum efficiency, a is the product of telescope collecting area and transmission, and α^2 is the area of night sky viewed by the detector.

$$SNR = \frac{\psi_{obj}\ a\ q\ t}{(\psi_{obj}\ a\ q\ t + \psi_{NSB}\ a\ q\ t\ \alpha^2)^{1/2}}$$

Solving for t,

$$t^{1/2} = \frac{SNR\ (\psi_{obj} a\ q\ t + \psi_{NSB} a\ q\ \alpha^2)^{1/2}}{\psi_{obj}\ aq}$$

$$t^{1/2} = \frac{SNR\ (\psi_{obj} + \psi_{NSB}\alpha^2)^{1/2}}{\psi_{obj} \cdot (aq)^{1/2}}$$

$$t = \frac{(SNR)^2}{(\psi_{obj})^2} \left[\frac{\psi_{obj} + \psi_{NSB}\alpha^2}{aq} \right]$$

For a range of object magnitudes and NSB's we calculate the integration times required to attain a SNR of 6.4. The results are given in Table II.

It can be seen from the data plotted in Figure 3 that for the range of NSB conditions considered, which are typical of those experienced at the GEODSS Experimental Test Site, measurements with the single cell radiometer require long integration times when the NSB level is high or when the object is very faint.

TABLE II

Integration times (t) required to achieve SNR = 6.4 for a range of object magnitudes and NSB for the GaAs photometer parameters described in the text. Note that the detector viewing area is 1250 arc-sec^2.

Object Magnitude	Integration Time (In Seconds) for NSB of			
	21^m/arc-sec^2	20^m/arc-sec^2	18^m/arc-sec^2	17.5^m/arc-sec^2
18^m	23.6	58.8	3.69×10^2	5.85×10^2
17^m	3.8	9.4	58.3	92.4
16^m	0.63	1.5	9.3	14.7
15^m	0.11	0.25	1.5	2.32
14^m	2.2×10^{-2}	4.4×10^{-2}	0.24	0.32
13^m	5.3×10^{-3}	8.8×10^{-3}	4×10^{-2}	6.1×10^{-2}
12^m	1.5×10^{-3}	2.1×10^{-3}	7×10^{-3}	1×10^{-2}

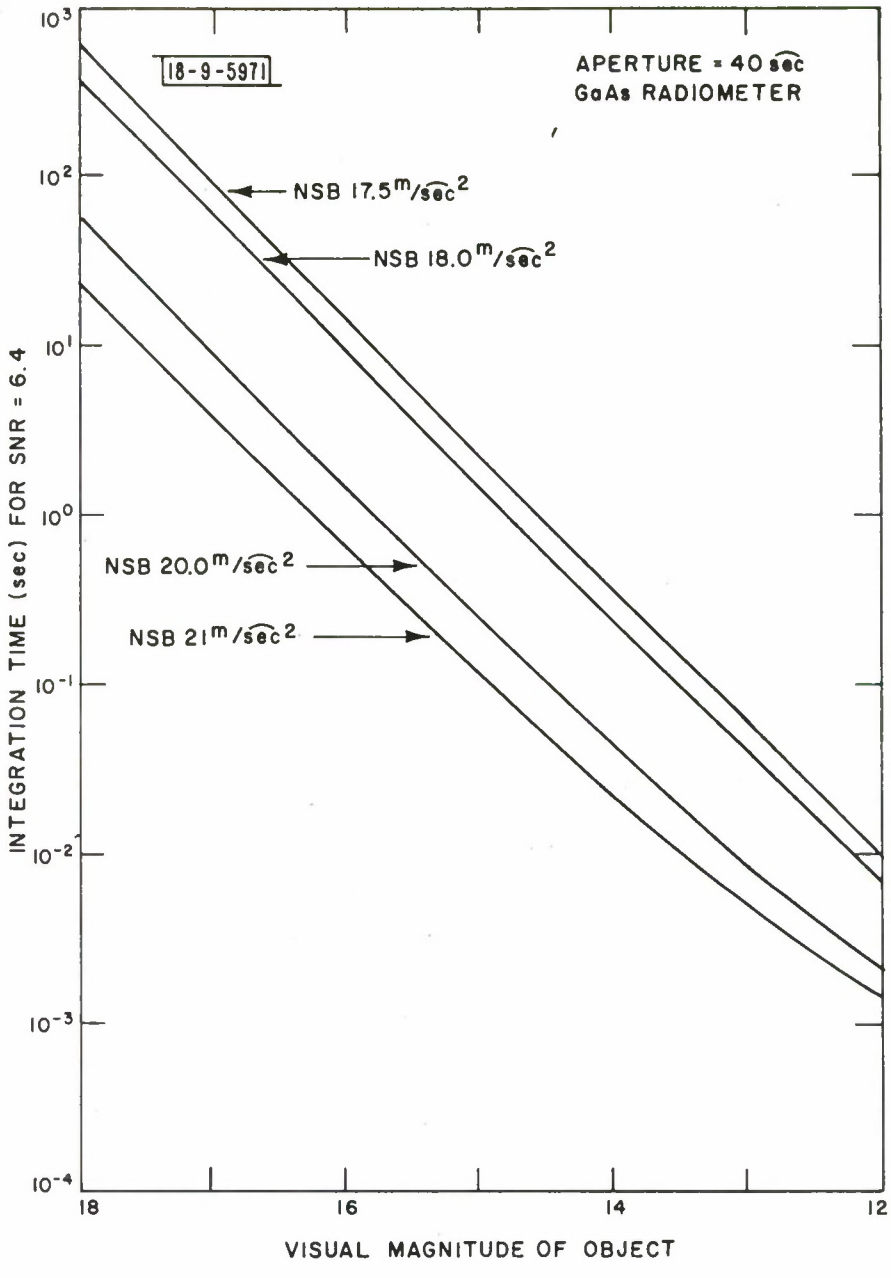

Fig. 3. Plot of Integration Time (t) required to achieve SNR = 6.4 with a GaAs photometer as a function of the visual magnitude of the object. NSB is the parameter. See text and Table II.

IV. MULTI-CHANNEL OR AREA RADIOMETER

For measuring faint sources an ideal single cell instrument would employ a spatial filter which matches the image shape of the source being measured and allows no additional background to fall on the detector. One way of achieving this is to use multiple cells, as shown in Figure 4. The background is reduced since outputs are combined only from those cells on which the image falls. This arrangement allows a simultaneous measurement of the sky background by sampling the outputs of cells not containing the image. This approach has the added advantage of doubling the time efficiency of the measurement.

As mentioned earlier, Wampler and Robinson at the Lick Observatory, University of California, have designed and built an instrument which attempts to accomplish the above. The technique, which has also been adopted by personnel at McDonald Observatory, uses three stages of image intensification followed by an image dissector tube which is the equivalent of a moving aperture (similiar to a flying spot scanner) which rapidly scans the field of view. This raster scan provides the equivalent of a multi-cell array. Photon events at a point in the field which occur between aperture samplings and which would be lost if a dissector tube (which has no built in memory) were used alone, are retained because of the slow decay time of the intensifier tube phosphor and are recorded on the next aperture scan.

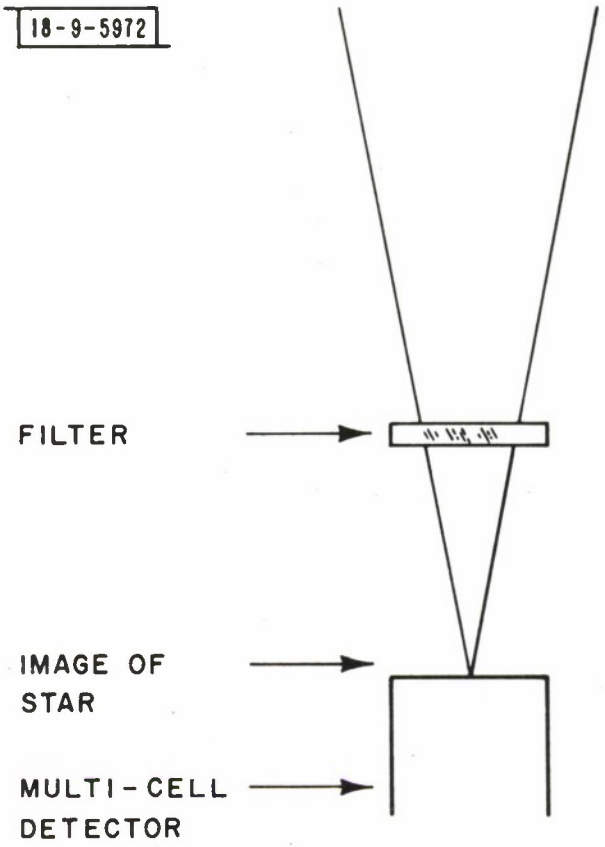

Fig. 4. Elements of an area radiometer.

This scheme solves the light storage problem between scans but introduces a new problem, phosphor afterglow, which can produce a contribution to the photon count for more than one aperture scan. In fact, bright sources which transit the field can produce a strong afterglow which contributes to the photon count for over an hour.

Attempts to analyze the afterglow problem analytically have met with only limited success because of the complicated nature of the phosphor decay mechanism.

V. CCD RADIOMETER

CCD devices with their built-in storage mechanism are ideally suited for use as a multi-cell or area radiometer. The requirements on the total number of elements required for the CCD array are modest (10^3 cells compared with 10^6 or 10^7 for most imaging applications) and are well within the current state of technology.

The Microelectronics Group at Lincoln Laboratory has a program for GEODSS to build a large array consisting of 100 x 400 element sections. Arrays of 30 x 30 cells have been built for testing and are available. We propose that a CCD area radiometer be designed and built with one of these arrays. A description of the proposed system follows.

The 30 x 30 cell devices have 1.2 x 1.2mil resolution cells so that the total width of the image area is 0.036 inch or slightly larger than the 30mil aperture now being used for the GaAs photometer. The device is designed to maximize the active area, the only inactive area being the channel stops (0.2mil wide) used to prevent blooming of strong signals across the columns. This imaging array, and the horizontal output register, operate with 2 phase clocks. The output register operates at frequencies which permit a data rate of 500kHz. At this data rate it takes

$$900 \times \frac{1}{5 \times 10^5} \text{ sec} = 1.8 \text{ milliseconds}$$

to read out the entire array.

Since the resolution cells of the array are 1.2mils square each cell sees

$$\phi = \frac{\ell}{f} = \frac{.0012}{155} \text{ rad} \times 57.3 \frac{\text{deg}}{\text{rad}} \times 3600 \frac{\text{arc-sec}}{\text{deg}} = 1.6 \text{ arc-sec}$$

in linear dimension, or 2.56 arc-sec^2 of the sky.

Although an idealized case, for an initial comparison let us examine the performance of the CCD array using the same telescope parameters as for the single cell above, assuming that the quantum efficiency is 0.4, that the noise term, N_I, can be neglected and the image is contained in a single cell (subsequently we will omit the latter two assumptions). Table III calculations are plotted in Figure 5, shows the required integration times to attain a SNR of 6.4.

Comparison of Figures 3 and 5 show the remarkable improvement in performance of the CCD array radiometer over the single cell radiometer. A more realistic situation is to omit the two assumptions made in calculating the data for Figure 5, i.e., 1) the electronic noise tern $N_I^2 = 0$ and 2) that the image is contained within a single cell. The electronic noise term N_I, while negligible for photomultipliers, must be included for CCD devices. The present CCD arrays being considered for this application have values of N_I ranging from 20 electrons for a quiet array (but not uncommon) to 100 electrons for a very noisy one. Only for excellent seeing conditions would the image be contained within a single cell. On a typical night suitable for making measurements, the diameter of the seeing disk is about 3 arc-seconds, and spreads over 4 cells. When seeing conditions get worse than this, experience at the GEODSS site has been that they get much worse.

Let us first include the N_I term and see its effect and then consider the multiple cell case. If we retain N_I, the equation for SNR becomes

TABLE III

Integration time (t) required to achieve SNR = 6.4 for a range of object magnitudes and NSB for a cell of the CCD radiometer described in the text. The same telescope parameters are used as in the calculation for Tables I and II.

Object Magnitude	Integration Time (In Seconds) For NSB of			
	21^m/arc-sec^2	20^m/arc-sec^2	18^m/arc-sec^2	17.5^m/arc-sec^2
18^m	0.13	0.16	0.39	0.56
17^m	4.7×10^{-2}	5.1×10^{-2}	8.9×10^{-2}	0.12
16^m	1.8×10^{-2}	1.9×10^{-2}	2.5×10^{-2}	2.9×10^{-2}
15^m	6.2×10^{-3}	7.2×10^{-3}	8.1×10^{-3}	8.8×10^{-3}
14^m	2.8×10^{-3}	2.9×10^{-3}	3.0×10^{-3}	3.1×10^{-3}
13^m	1.1×10^{-3}	1.1×10^{-3}	1.1×10^{-3}	1.2×10^{-3}
12^m	4.4×10^{-4}	4.4×10^{-4}	4.4×10^{-4}	4.5×10^{-4}

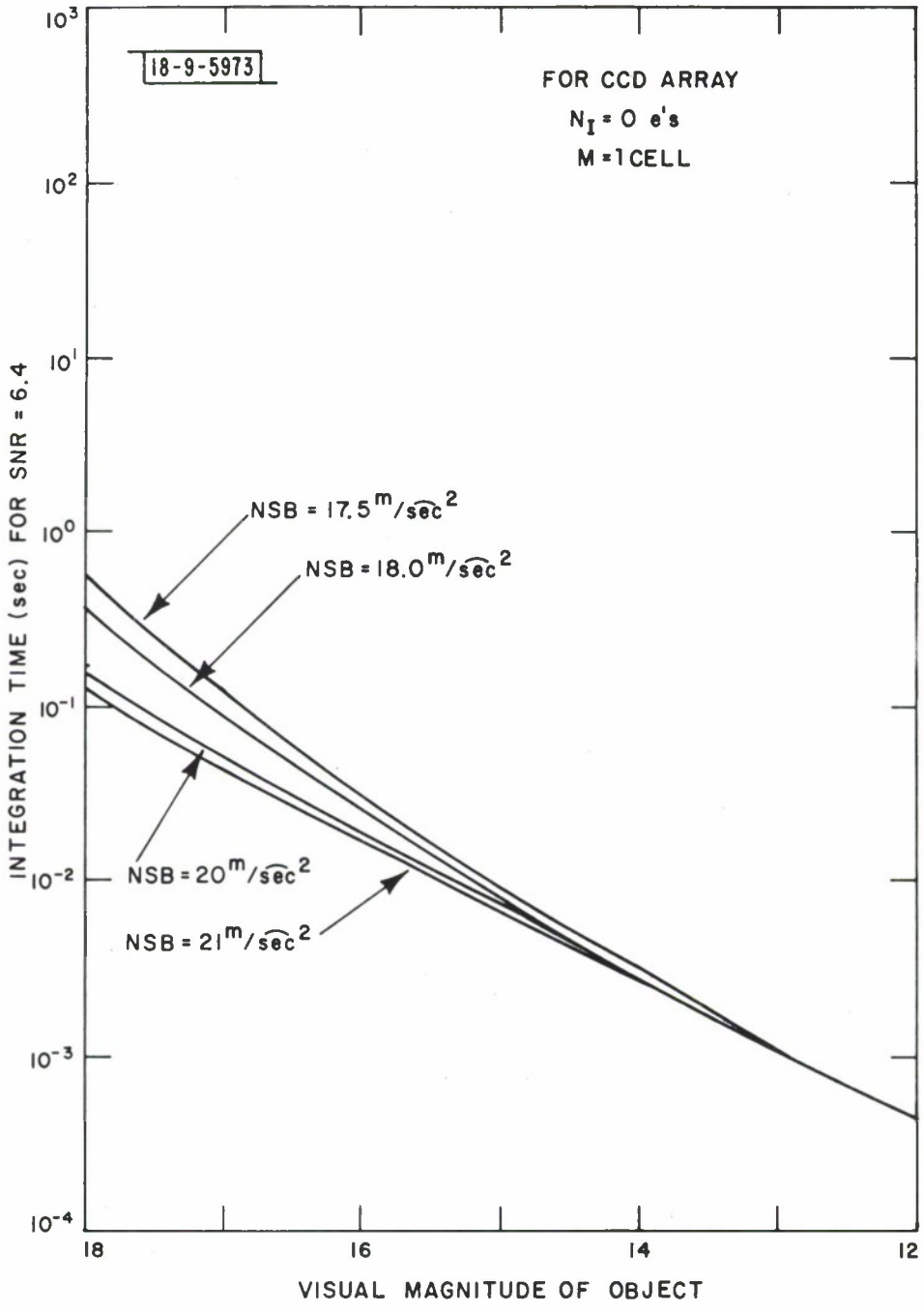

Fig. 5. Plot of Integration Time (t) required to achieve SNR = 6.4 with a single cell noiseless CCD imager as a function of the object visual magnitude. NSB is the parameter. See text and Table III.

$$SNR = \frac{\psi_{obj} aqt}{\left[\psi_{obj} aqt + \psi_{NSB} aqt\alpha^2 + N_I^2\right]^{1/2}}$$

Since N_I is associated with the cell read out, to a first approximation it is independent of the integration time, t.

$$(SNR)^2 \left[\psi_{obj}\, aqt + \psi_{NSB}\, aq\alpha^2\, t + N_I^2\right] = \psi^2_{obj} a^2 q^2 t^2$$

$$\psi^2_{obj} a^2 q^2 t^2 - \left[(SNR)^2 \psi_{obj} aq + (SNR)^2 \psi_{NSB} aq\alpha^2\right] t - (SNR)^2 N_I^2 = 0$$

$$t = \frac{\left[(SNR)^2 \psi_{obj} aq + (SNR)^2 \psi_{NSB} aq\alpha^2\right]}{2\psi^2_{obj} a^2 q^2}$$

$$\pm \frac{\left\{\left[(SNR)^2 \psi_{obj} aq + (SNR)^2 \psi_{NSB} aq\alpha^2\right]^2 + \left[4\psi^2_{obj} a^2 q^2 (SNR)^2 N_I^2\right]\right\}^{1/2}}{2\psi^2_{obj} a^2 q^2}$$

$$t = \frac{(SNR)^2}{2\psi^2_{obj} aq} \left\{\left[\psi_{obj} + \psi_{NSB}\alpha^2\right] \pm \left[\left(\psi_{obj} + \psi_{NSB}\alpha^2\right)^2 + \frac{4\psi^2_{obj} N_I^2}{(SNR)^2}\right]^{1/2}\right\}$$

For SNR = 6.4, the expression becomes

$$t = \frac{174}{\psi_{obj}} 2 \left\{ \left(\psi_{obj} + \psi_{NSB}\alpha^2 \right) \pm \left[\left(\psi_{obj} + \psi_{NSB}\alpha^2 \right)^2 + 0.1\psi_{obj}{}^2 N_I{}^2 \right]^{1/2} \right\}$$

The effect of retaining the N_I term is shown in the data in Table IV which is plotted as Figure 6. A family of curves for different values of NSB is shown for N_I = 20 electrons and N_I = 100 electrons.

As expected the addition of electron noise increases the required integration time. However, a comparison of Figure 6 with Figure 3 shows that the small area detectors have a significant advantage over the large area ones.

Let us now consider the case where the image is contained on M cells rather than on a single cell. The total photoelection count, ϕ_e, is obtained by summing the contribution from the M cells containing the signal,

$$\phi_e = \sum_{i=1}^{M} \phi_{e_i} = \sum \psi_{obj_i} aqt$$

If ϕ_{NSB_i} and N_{I_i} are the detected photoelectron count noise contributions associated with $i^{\underline{th}}$ cell from night sky background and electronic read-out noise respectively the expression for the SNR becomes

$$SNR = \frac{\sum_{i=1}^{M} \psi_{obj_i} aqt}{\left[\sum_{i=1}^{M} \left(\psi_{obj_i} aqt + \psi_{NSB_i} aq\alpha^2 t + N_{I_i}^2 \right) \right]^{1/2}}$$

TABLE IV

Same as Table III except that the integration times are calculated assuming values of N_I = 20 and N_I = 100 for the CCD readout noise.

Object Magnitude	Integration Time in Seconds for NSB of			
	21^m/arc-sec^2	20^m/arc-sec^2	18^m/arc-sec^2	17.5^m/arc-sec^2
For N_I = 20 e's				
18^m	0.42	0.44	0.60	0.73
17^m	0.16	0.17	0.19	0.21
16^m	6.5×10^{2}	6.6×10^{2}	6.9×10^{-2}	7.2×10^{-2}
15^m	2.6×10^{-2}	2.6×10^{-2}	2.7×10^{-2}	2.7×10^{-2}
14^m	1×10^{-2}	1×10^{-2}	1×10^{-2}	1×10^{-2}
13^m	4.1×10^{-3}	4.1×10^{-3}	4.1×10^{-3}	4.1×10^{-3}
12^m	1.6×10^{-3}	1.6×10^{-3}	1.6×10^{-3}	1.6×10^{-3}
For N_I = 100 e's				
18^m	1.81	1.83	1.95	2.1
17^m	0.72	0.72	0.74	0.76
16^m	0.29	0.29	0.29	0.29
15^m	0.14	0.14	0.14	0.14
14^m	4.5×10^{-2}	4.5×10^{-2}	4.5×10^{-2}	4.5×10^{-2}
13^m	1.8×10^{-2}	1.8×10^{-2}	1.8×10^{-2}	1.8×10^{-2}
12^m	7.2×10^{-3}	7.2×10^{-3}	7.2×10^{-3}	7.2×10^{-3}

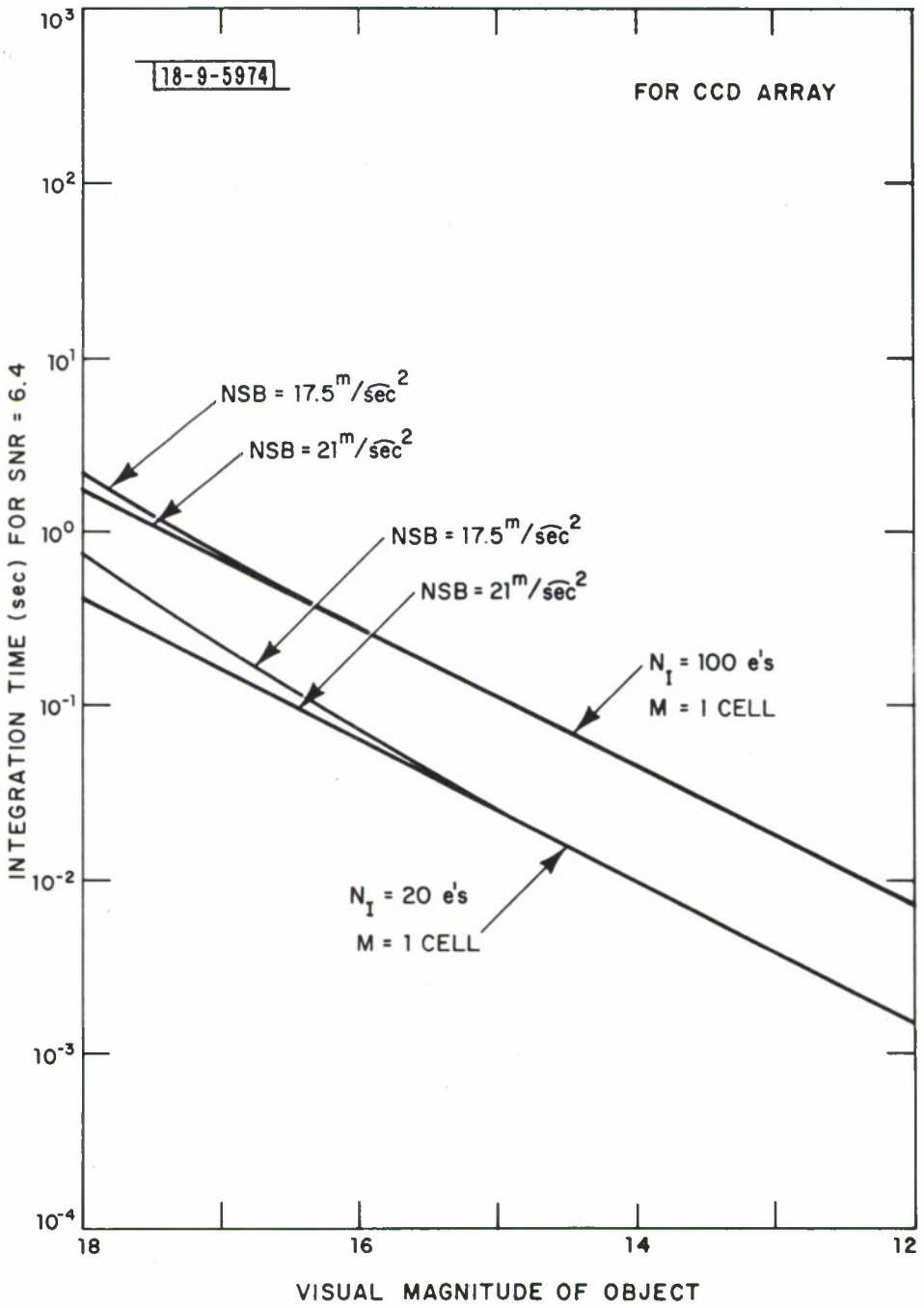

Fig. 6. Plot of Integration Time (t) required to achieve SNR = 6.4 with a single cell imager as a function of the object visual magnitude. NSB and electron readout noise are the parameters. See text and Table IV.

If we now assume that all of the signal is recovered

$$\sum_{i=1}^{M} \psi_{obj_i} aqt = \psi_{obj} aqt$$

and that the background and noise readouts are the same for all cells

$$\sum_{i=1}^{M} \psi_{NSB_i} aq\alpha^2 t = M\psi_{NSB} aq\alpha^2 t \quad \text{and}$$

$$\sum_{i=1}^{M} N_{I_i}^2 = M\, N_I^2.$$

The SNR reduces to

$$SNR = \frac{\psi_{obj}\, aqt}{\left[\psi_{obj} aqt + M\psi_{NSB} aq\alpha^2 t + M\, N_I^2\right]^{1/2}}$$

It is the same expression as for the single cell except that the noise contributions from ψ_{NSB} and N_I have been multiplied by M, the number of cells over which the image is spread.

Let us take the example in which the blur circle diameter due to seeing conditions is 3 arc-seconds, so that the signal is spread over a total of four cells and the NSB and N_I noises are increased proportionally.

The integration times for a range of object magnitudes and values of NSB are given in Table V for N_I = 20 electrons and N_I = 100 electrons. These calculations are plotted in Figure 7 and show that the net effect of spreading the image over four cells is to approximately double the integration time.

Let us now compare the performance of the CCD and GaAs devices under operating conditions encountered in a field environment. The first factor that should be included is atmospheric transmission which at the Experimental Test Site (ETS) at New Mexico is about 0.8 for one air mass. However, the objects being measured are not usually positioned overhead so that we have chosen 0.7 as a typical value for the atmospheric transmission. This value is used to calculate the data plotted in Figures 8 and 9. We have plotted an additional curve for the GaAs radiometer, one showing the performance of the device with a 20 arc-sec aperture which we consider a limiting case for the GEODSS telescope when tracking objects which are moving at non-sidereal rates. For the CCD device we have plotted curves for two values of electronic noise N_I = 20 electrons which we feel is indicative of what is achievable and N_I = 100 electrons which we consider a "worst case" situation.

Figures 8a and b show a comparison of the GaAs and CCD radiometers for bright and dark night sky background conditions respectively. For all satellite brightnesses considered, against a high level of NSB, the CCD radiometer with N_I = 20 electrons requires shorter integration times than the GaAs radiometer even for the 20 arc-sec aperture. Against dark

TABLE V

Same as Table III, except that readout noise (N_I = 20 and 100) and the object signal is spread out over 4 cells.

Object Magnitude	Integration Time (In Seconds) For NSB of			
	21^m/arc-sec^2	20^m/arc-sec^2	18^m/arc-sec^2	17.5^m/arc-sec^2
Case I M = 4				
18^m	0.80	0.86	1.6	2.1
17^m	0.31	0.32	0.41	0.49
16^m	0.12	0.12	0.14	0.15
15^m	4.8×10^{-2}	4.8×10^{-2}	5.0×10^{-2}	5.2×10^{-2}
14^m	1.9×10^{-2}	1.9×10^{-2}	1.9×10^{-2}	2.0×10^{-2}
13^m	7.6×10^{-3}	7.6×10^{-3}	7.6×10^{-3}	7.6×10^{-3}
12^m	3.0×10^{-3}	3.0×10^{-3}	3.0×10^{-3}	3.0×10^{-3}
Case II M = 4				
18^m	3.5	3.6	4.2	4.6
17^m	1.4	1.4	1.5	1.6
16^m	0.56	0.56	0.58	0.59
15^m	0.22	0.22	0.23	0.23
14^m	8.9×10^{-2}	8.9×10^{-2}	8.9×10^{-2}	8.9×10^{-2}
13^m	3.5×10^{-2}	3.6×10^{-2}	3.6×10^{-2}	3.6×10^{-2}
12^m	1.4×10^{-2}	1.4×10^{-2}	1.4×10^{-2}	1.4×10^{-2}

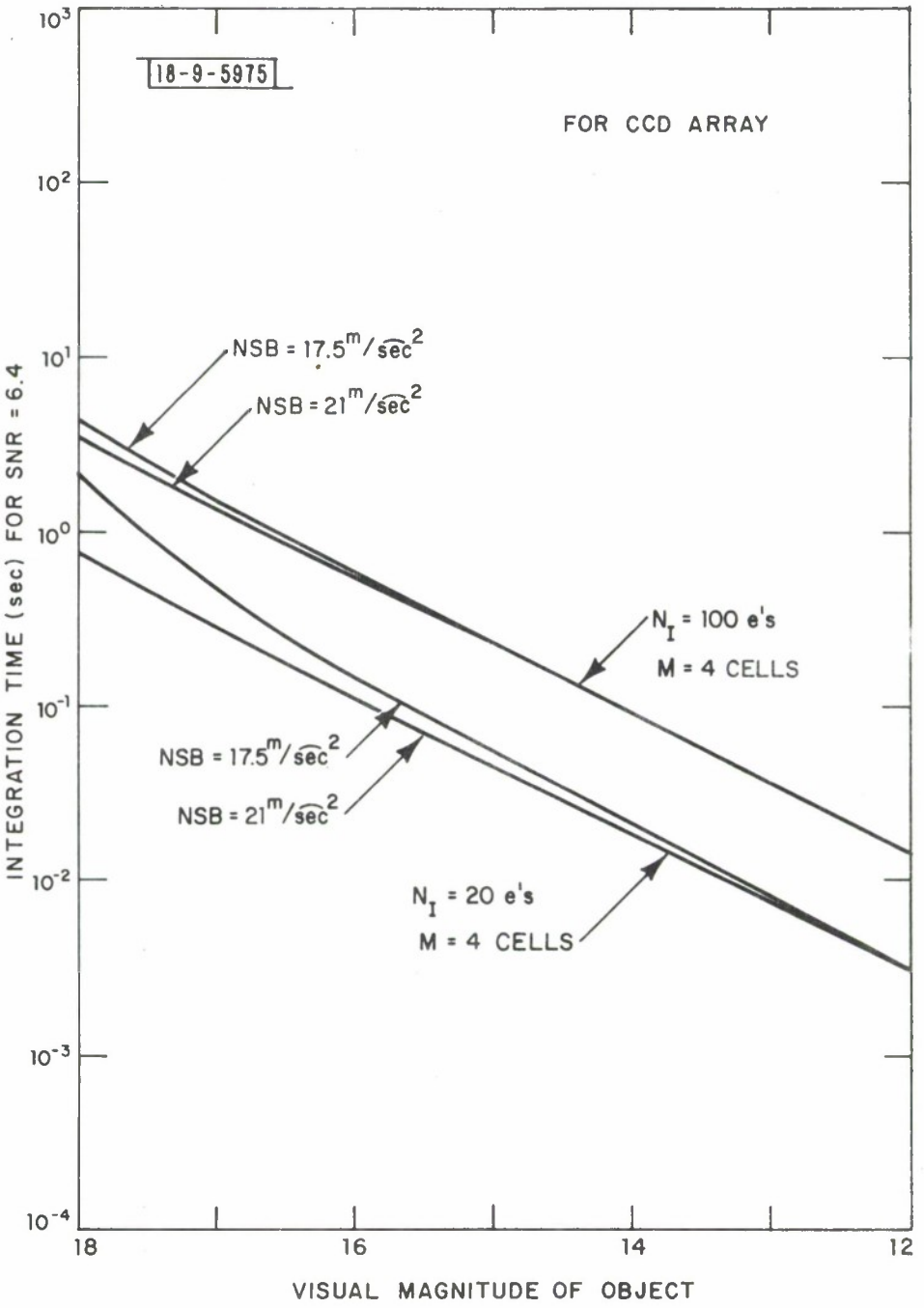

Fig. 7. Plot of Integration Time (t) required to achieve SNR = 6.4 with a 4 cell CCD imager as a function of the object visual magnitude. NSB and electron readout noise are the parameters. See text and Table V.

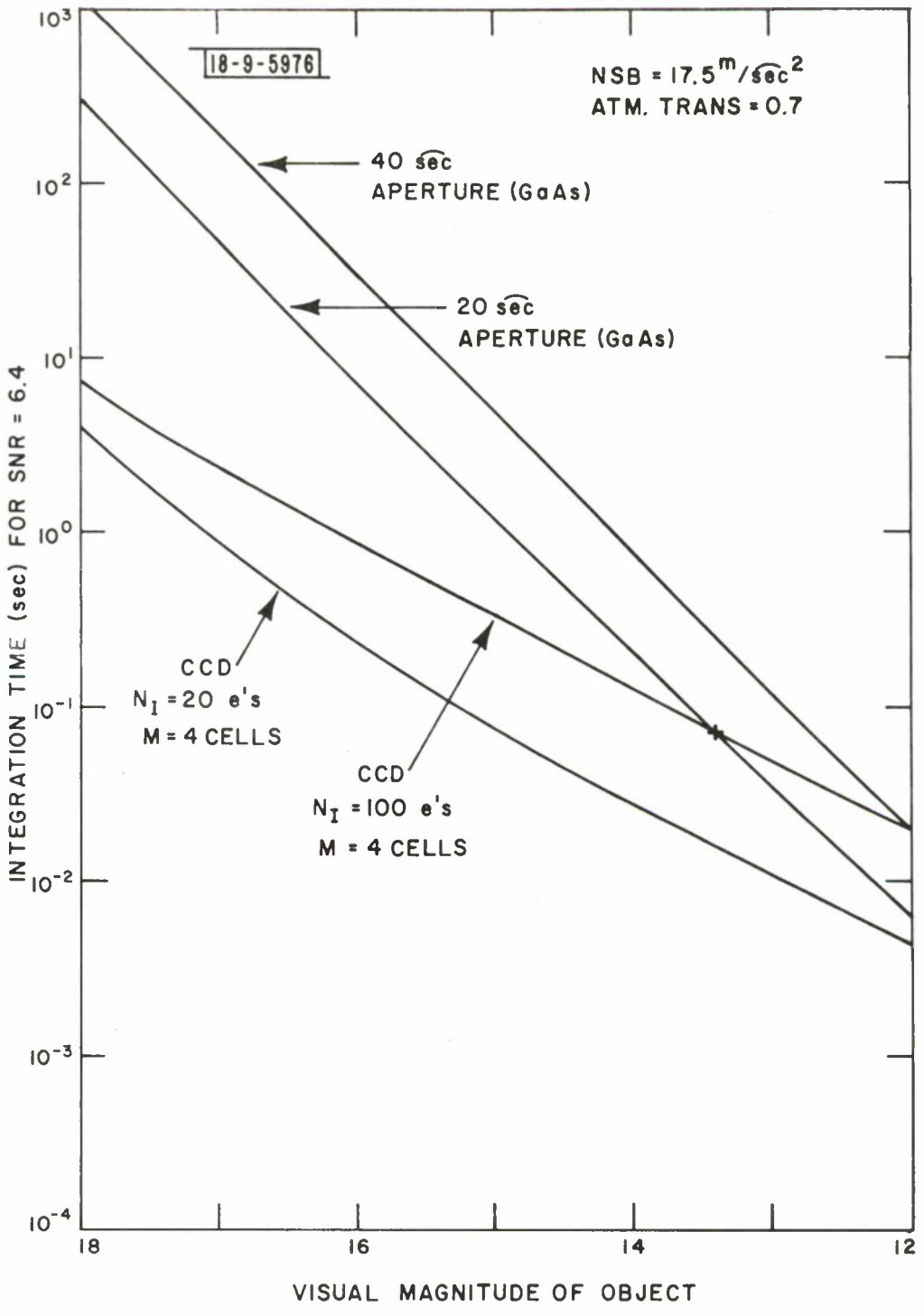

Fig. 8a. A comparison of the GaAs large aperture photometer with a 4 cell small aperture CCD imager for bright night sky.

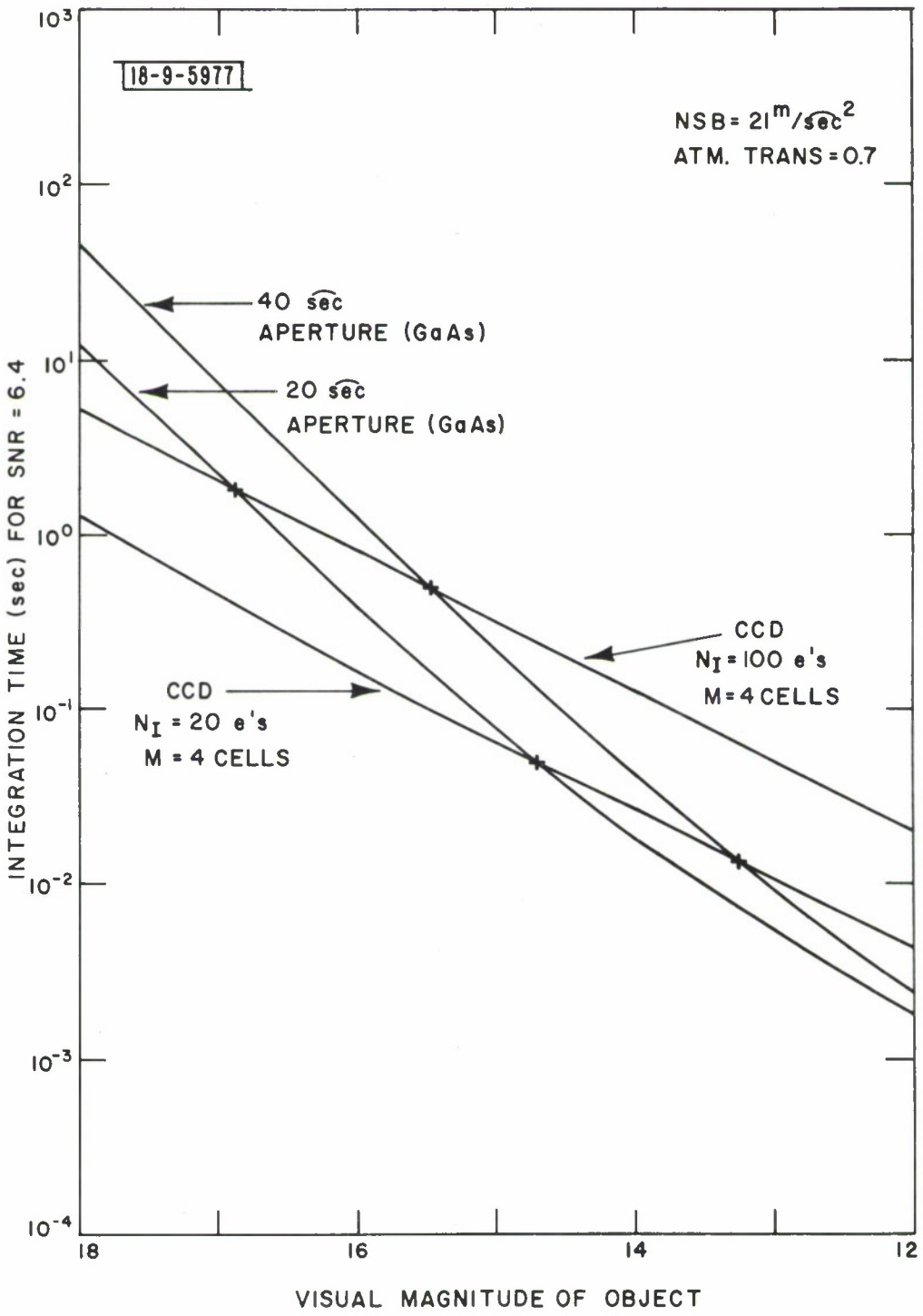

Fig. 8b. Same as Fig. 8a, except for dark night sky background.

sky conditions, the CCD radiometer (N_I = 20 electrons) outperforms the GaAs radiometer for objects fainter than 13.3^m and 14.7^m for the 40 arc-sec and 20 arc-sec design, respectively.

In an operational situation the radiometer must be continually pointed at the object on which data is being collected. The CCD array can be made to self track but the GaAs radiometer does not have this feature and must be pointed by a separate instrument. The present design for the GaAs radiometer uses a pellicle to divide the light from the telescope equally between the radiometer and the tracking instrument in the ratio of 40% and 40% with 20% being lost in the pellicle. This means that when employed in an operational situation the GaAs receives only (0.6) (0.4) or 24% of the light incident on the telescope compared with 60% for the CCD array, or a difference of one magnitude. Figures 9a and b, compare the two devices in an operational configuration for bright and dark night sky conditions. Under this condition the CCD radiometer outperforms even the 20 arc-sec GaAs design for the entire range of NSB levels and satellite magnitudes considered.

For convenience, a short summary of the required integration times for the two devices is given in Table VI.

Although there are many ways in which the signal from the CCD imaging radiometer can be processed, the following is a technique which appears to satisfy the signal processing requirements.

Figure 10 is a photograph of the 30 x 30 element array. Also seen in the photograph are the input and output CCD registers, and the input and output devices for testing with electrical inputs. Note that in the

TABLE VI

Ratio of t's required by GaAs vs the CCD array (N_I = 20 e's, M = 4 cells) for different sky conditions.

Sky	Bright (17.5^m/arc-sec^2)		Dark (21^m/arc-sec^2)	
Object	Dim (18^m)	Bright (12^m)	Dim (18^m)	Bright (12^m)
GaAs (40 arc-sec)	206X	3.5X	29X	0.5X
GaAs (20 arc-sec)	52X	1.2X	7.6X	0.4X
GaAs (40 arc-sec) 40% Beam sharing	519X	8.6X	73X	1.3X
GaAs (20 arc-sec) 40%Beam sharing	130X	22X	183X	3.3X

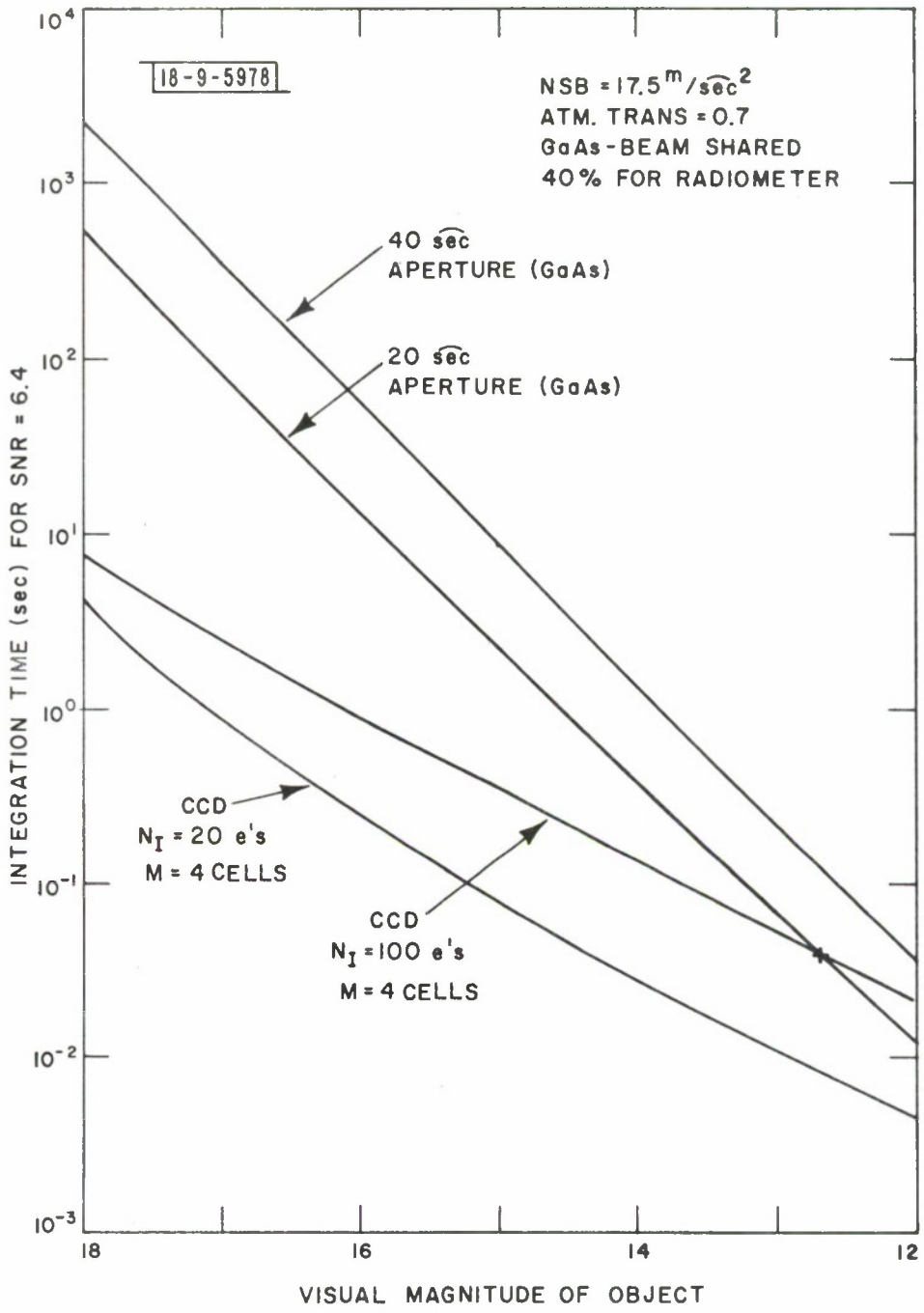

Fig. 9a. A comparison in an operational situation (tracking required) of the GaAs Large aperture photometer with a 4 cell small aperture CCD imager for bright night sky.

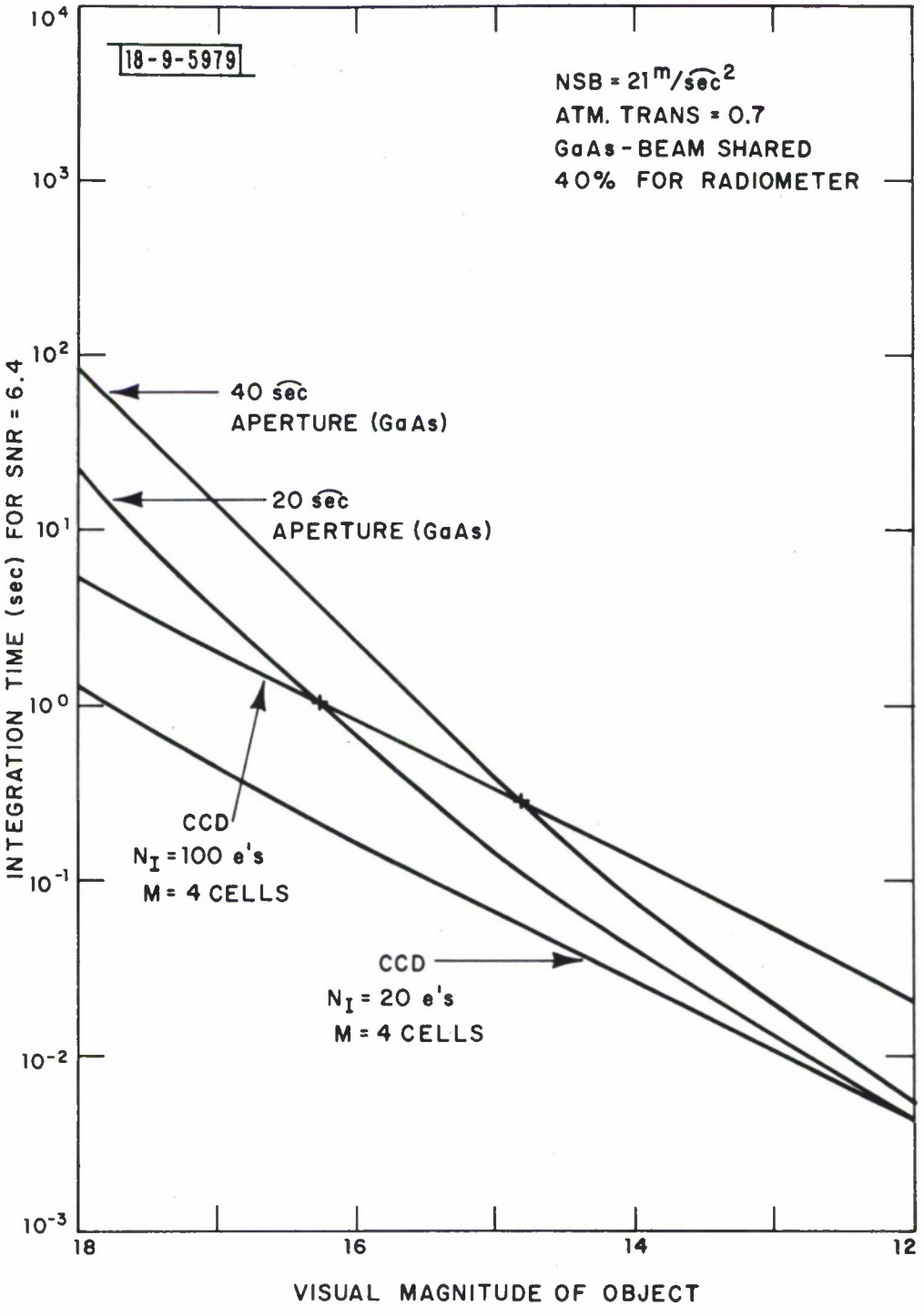

Fig. 9b. Same as Fig. 9a, except for dark night sky background.

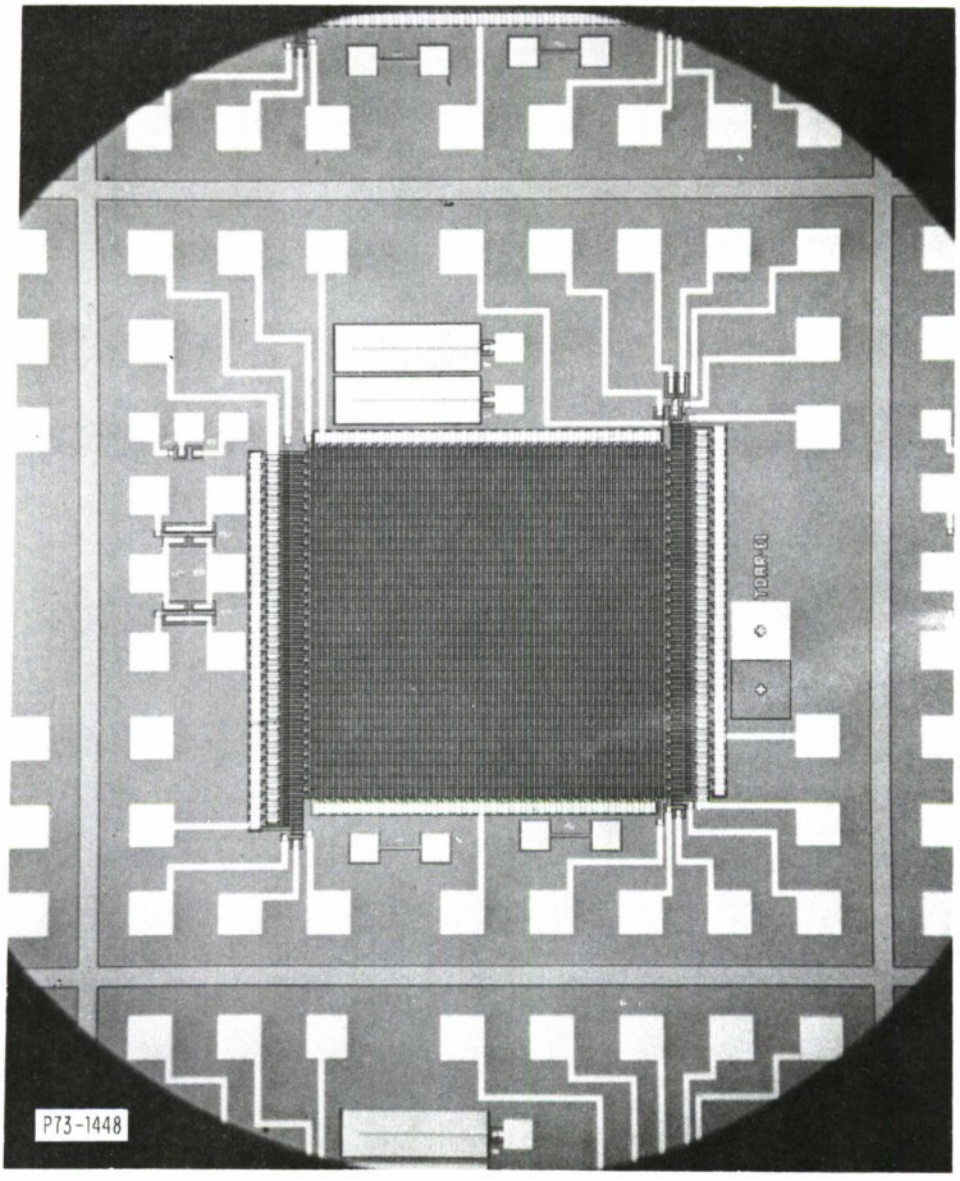

Fig. 10. Photograph of a 30 x 30 element array.

devices as fabricated there is no light shield over the input and output registers. For use as a radiometer, the light shield could be an aperture placed either on the surface of the array, or immediately above it. If the aperture were made slightly smaller than the array, the darkened cells could be used to measure the electrical readout noise of the device.

To process the data, a set of 6 buffers 34 cells long (the input and output registers are 34 cells long to allow for, and make sure of, the zeroing of the signal between samples) is required. When the readout of the first (bottom) row of the array begins, a peak detector is set to zero, and the row is saved in the first buffer. The peak detector is used to store the peak value in that row, and a counter is used to store its location. A flag is also set to indicate that the largest signal has occurred in this row.

There are 3 flags for each buffer, and each buffer is associated with a counter which reads from 1 to 30. Flag 1 on indicates that the peak signal occurred on that row; flag 2 on is used to indicate the rows just preceding and following the row containing the peak signal; and flag 3 on is used to indicate the row about to be read. Flags on all the other rows are set off.

Then, when the first (bottom) row is read out, the first buffer is numbered 1, and the second buffer is numbered 2. As the signal samples are read in the flags are set as above. Any unflagged buffer is available for the next row to be read in. In this manner, only the 3 rows containing

the peak signal and the two adjacent rows are retained for data processing. If row 30 is covered by a light shield, and flags associated with it set off, it can conveniently be used for the readout noise evaluation.

When the location of the peak signal is known, the data processing can be carried out by using the peak signal, and adding to it, the signal from as many adjacent cells as desired. As indicated earlier, the signal from the night sky background and the noise readout can be ascertained from the remaining cells. One, thus, has all the information necessary for signal evaluation.

It should be noted that, except for the shortest sampling times, there should be sufficient time for data processing between sample readouts.

VI. SUMMARY AND RECOMMENDATIONS

Following is a summary of the advantages of the proposed CCD radiometer, including some which have not been mentioned in the above analysis.

(1) In general, the CCD provides a significant improvement in the integration time required to measure the intensity of objects. Not only is the time of a measurement reduced significantly and the telescope used more efficiently, but data with finer time resolution can be obtained on sources whose intensity fluctuations are of interest.

(2) Measurements of the sky background can be measured simultaneously with the signal. This halves the time of a measurement compared to a PMT type radiometer, which requires an independent measurement of this quantity.

(3) The fact that an array of cells is used permits a number of real time data processing options to be designed into the system. Some examples are given below.

(a) The device can be used as a closed loop tracker to point the telescope and the entire telescope output used by the radiometer. Tracking is accomplished by generating an error signal which is proportional to the distance from the center of gravity of the image to a reference point on the raster, for example the center cell of the array.

(b) By monitoring the count from the cells on the perimeter of the array, it is possible to design "star guards" or "star alerts" which automatically detect the presence of stars entering the field of view of the instrument. Data collected during these periods can be tagged and deleted from the reduction process if desired.

(c) By a variation of the technique above, clouds and regions of poor atmospheric transmission can be detected and the data rejected.

(d) By shielding a small area, say along an edge of the CCD array, from the incident light, a measure of the readout noise can be made. This means that the object signal, the signal due to NSB and the readout noise can all be measured at the same time.

(e) The signal can be displayed on a video monitor for real time observation of the object in the aperture of the radiometer.

(4) Finally, employing CCD technology should result in a stable, long life instrument. Eliminating the need for high voltages can be considered a plus.

We recommend that a program be initiated to test in the laboratory a 30 x 30 cell CCD array for utilization as a radiometer for the GEODSS. Laboratory tests should be followed by thorough field testing at the ETS.

APPENDIX A

PHOTOELECTRON COUNTS

Tables A - I and A - II give the photoelectron counts used in the text for the following parameters:

TELESCOPE

Collecting Area = $0.49m^2$

Optical Losses = 40%

GaAs DETECTOR

Quantum Efficiency = 15%

Aperture #1 = 40 arc-sec

Sky Area Subtended, α_1^2 = 1250 $arc\text{-}sec^2$

Aperture #2 = 40 arc-sec

Sky Area Subtended, α_2^2 = 314 $arc\text{-}sec^2$

CCD ARRAY

Quantum Efficiency = 40%

Sky Subtended/Resel, α^2 = 2.56 $arc\text{-}sec^2$

ATMOSPHERE

No Loss

ZERO MAGNITUDE REFERENCE

5×10^{10} photons/sec/m^2 for $M_v = 0$

TABLE A - I

PHOTOELECTRON COUNTS USING GaAs DETECTOR

Target Magnitude	Signal Counts/Sec	NSB Level	Aperture #1 NSB Counts/Sec	Aperture #2 NSB Counts/Sec
18^m	139	$22^m/arc\text{-}sec^2$	4.37×10^3	1.1×10^3
17^m	350	$21^m/arc\text{-}sec^2$	1.1×10^4	2.76×10^3
16^m	878	$20^m/arc\text{-}sec^2$	2.76×10^4	6.94×10^3
15^m	2.21×10^3	$19^m/arc\text{-}sec^2$	6.92×10^4	1.74×10^4
14^m	5.54×10^3	$18^m/arc\text{-}sec^2$	1.74×10^5	4.36×10^4
13^m	1.39×10^4	$17.5^m/arc\text{-}sec^2$	2.76×10^5	6.94×10^4
12^m	3.50×10^4			

TABLE A - II

PHOTOELECTRON COUNTS USING CCD ARRAY DETECTOR
WITH IMAGE FOCUSED ON A SINGLE RESEL

Target Magnitude	Signal Counts/Sec	NSB Level	NSB Counts/resel/sec
18^m	371	$22^m/\text{arc-sec}^2$	23.9
17^m	932	$21^m/\text{arc-sec}^2$	60.
16^m	2.34×10^3	$20^m/\text{arc-sec}^2$	151.
15^m	5.88×10^3	$19^m/\text{arc-sec}^2$	378
14^m	1.48×10^4	$18^m/\text{arc-sec}^2$	948
13^m	3.71×10^4	$17.5^m/\text{arc-sec}^2$	1.51×10^3
12^m	9.32×10^4		

REFERENCES

1. L. B. Robinson E. J. Wampler, "The Lick Observatory Image - Dissector Scanner," Pub. Astron. Soc. Pacific, 84 (1972).

2. J. McNall et al., "The Response of Phosphor - Output Image Intensifiers to Single-Photon Inputs, " Pub. Astron. Soc. Pacific, 82, No. 488 (1970).

3. R. E. Nather, "Multi-Channel Area Photometer," Pub. Astron. Soc. Pacific, 84 (1972).

4. Department of Astronomy and McDonald Observatory, University of Texas, "Digital Area Photometer 100 DAC Report" (25 July 1974), AF Contract F04701-74-C-0317.

5. R. Weber, "Visual Magnitude Flux Rate Density Standards for Sunlight Incident on Photoemissive Surfaces," Technical Note 1974-20, Lincoln Laboratory, M.I.T. (6 May 1974), DDC AD-779822/6.

6. R. Weber, "The Detection Capabilities of Gallium Arsenide and S-20 Photo-Multiplier Tubes to GO - Type, Point-Source, Signals," Technical Note 1976-13, Lincoln Laboratory, M.I.T. (3 March 1976), DDC AD-A023818/8.

ACKNOWLEDGEMENTS

We would like to thank Robert J. Bergemann for many useful discussions and suggestions, W. J. Taylor for discussions on signal processing techniques, and John Sorvari for discussions of the problems concerning radiometric measurements. If the techniques suggested in this Note give useful results, many of his suggestions will undoubtedly be incorporated in future versions of the radiometer.

UNCLASSIFIED

SECURITY CLASSIFICATION OF THIS PAGE *(When Data Entered)*

REPORT DOCUMENTATION PAGE		READ INSTRUCTIONS BEFORE COMPLETING FORM
1. REPORT NUMBER ESD-TR-77-280	2. GOVT ACCESSION NO.	3. RECIPIENT'S CATALOG NUMBER
4. TITLE *(and Subtitle)* A CCD Radiometer for Use in GEODSS		5. TYPE OF REPORT & PERIOD COVERED Project Report 6. PERFORMING ORG. REPORT NUMBER Project Report ETS-25
7. AUTHOR*(s)* Frank L. McNamara and William E. Krag		8. CONTRACT OR GRANT NUMBER*(s)* F19628-78-C-0002
9. PERFORMING ORGANIZATION NAME AND ADDRESS Lincoln Laboratory, M.I.T. P.O. Box 73 Lexington, MA 02173		10. PROGRAM ELEMENT, PROJECT, TASK AREA & WORK UNIT NUMBERS Program Element No. 63428F Project No. 2128
11. CONTROLLING OFFICE NAME AND ADDRESS Air Force Systems Command, USAF Andrews AFB Washington, DC 20331		12. REPORT DATE 4 November 1977 13. NUMBER OF PAGES 50
14. MONITORING AGENCY NAME & ADDRESS *(if different from Controlling Office)* Electronic Systems Division Hanscom AFB Bedford, MA 01731		15. SECURITY CLASS. *(of this report)* Unclassified 15a. DECLASSIFICATION DOWNGRADING SCHEDULE

16. DISTRIBUTION STATEMENT *(of this Report)*

Approved for public release; distribution unlimited.

17. DISTRIBUTION STATEMENT *(of the obstroct entered in Block 20, if different from Report)*

18. SUPPLEMENTARY NOTES

None

19. KEY WORDS *(Continue on reverse side if necessary and identify by block number)*

CCD radiometer	White Sands	optical signature
GEODSS	satellite brightness	telescope

20. ABSTRACT *(Continue on reverse side if necessary and identify by block number)*

Proposed is a CCD radiometer for application in the GEODSS Program. An analysis is made of the predicted performance in a field environment. The results are compared for a variety of satellite brightnesses and levels of night sky background with the present single cell GaAs radiometer undergoing tests at the GEODSS Experimental Test Facility at White Sands Missile Range, New Mexico and with the Robinson-Wampler multi-channel radiometer in use at Lick Observatory, University of California, Santa Cruz, California, and the McDonald Observatory, University of Texas, Fort Davis, Texas. The comparison indicates that the CCD radiometer allows the optical signature of objects to be determined with higher accuracy and improved time resolution, and permits a more efficient utilization of telescope time.

DD FORM 1 JAN 73 1473 EDITION OF 1 NOV 65 IS OBSOLETE

UNCLASSIFIED

SECURITY CLASSIFICATION OF THIS PAGE *(When Data Entered)*